Supplementary Information

Ultralarge Modulation of Fluorescence by Neuromodulators in Carbon Nanotubes Functionalized with Self-assembled Oligonucleotide Rings

Abraham G. Beyene,[1,‡] Ali A. Alizadehmojarad,[2,†,‡] Gabriel Dorlhiac,[3] Natalie Goh,[1] Aaron M. Streets,[3,4,5] Petr Král,[6] Lela Vuković,[2,], and Markita P. Landry[1,5,7,*]*

[1] Department of Chemical and Biomolecular Engineering, University of California, Berkeley, Berkeley, CA 94720

[2] Department of Chemistry and Biochemistry, University of Texas at El Paso, El Paso, TX 79968

[3] Berkeley Biophysics Program, University of California, Berkeley, Berkeley, CA 94720

[4] Department of Bioengineering, University of California, Berkeley, Berkeley, CA 94720

[5] Chan-Zuckerberg Biohub, San Francisco, CA 94158

[6] Department of Chemistry, Physics, and Biopharmaceutical Sciences, University of Illinois at Chicago, Chicago, IL 60607

[7] California Institute for Quantitative Biosciences (qb3), University of California, Berkeley, Berkeley, CA 94720

Materials and Methods

Suspension of SWNT in ssDNA

All ssDNA oligonucleotides were purchased from Integrated DNA Technologies (Standard Desalting). HiPCo SWNT were purchased from NanoIntegris (Batch # HR27-104). Each ssDNA-SWNT colloidal suspension was prepared by mixing 1 mg of ssDNA and 2 mg of SWNT in 1 mL of 100 mM NaCl solution. The solution was bath sonicated (Branson Ultrasonic 1800) for 10 minutes and probe-tip sonicated for 10 minutes at 5 W power (Cole Parmer Ultrasonic Processor, 3 mm tip diameter) in an ice-bath. The sonicated solution was incubated at room temperature for 30 minutes. The product was subsequently centrifuged at 16,000 g (Eppendorf 5418) for 90 minutes to remove unsuspended SWNT bundles and amorphous carbon, and the supernatant was recovered for further characterization. To vary ssDNA SWNT surface packing, we used 2 mg, 5 mg, or 10 mg of starting SWNT masses in 1 mg of $(GT)_6$ dissolved in 100 mM NaCl.

Characterizations of SWNT-ssDNA suspensions

All absorption measurements were taken with a UV-VIS-NIR spectrophotometer (Shimadzu UV-3600 Plus) or UV-VIS (ThermoFisher Scientific Genesys 20). SWNT concentrations of as-made ssDNA-SWNT suspensions were determined using absorbance at 632 nm (UV-VIS) and extinction coefficient of $\varepsilon = 0.036\ (mg/L)^{-1}\ cm^{-1}$.[1] Full spectrum absorbance measurements were recorded with UV-VIS-NIR after dilution to 5 mg/L SWNT concentration in 100 mM NaCl. For fluorescence measurements, each suspension was diluted to 5 mg/L in 100 mM NaCl and aliquots of 198 μL volume were placed in each well of a 96-well plate (CORNING). Fluorescence measurements were obtained with a 20X objective on an inverted Zeiss microscope

(Axio Observer.D1) coupled to a Princeton Instruments spectrometer (SCT 320) and liquid nitrogen cooled Princeton Instruments InGaAs detector (PyLoN-IR). A 721 nm laser (OptoEngine LLC) was used as the excitation light source. To investigate solution ionic strength, $(GT)_6$-SWNT suspensions were diluted to 5 mg/L in 1 mM, 10 mM, 50 mM, 100 mM, and 200 mM NaCl solution and allowed to incubate for 24 hrs. before fluorescence measurements were taken. pH adjustments were made using HCl or NaOH and fluorescence measurements were taken after 1 hr. equilibration at room temperature. We used 2 s exposure times at laser power of 65 mW for most measurements. In very bright SWNT suspensions, exposure times were reduced to 0.5 s or 1 s and fluorescence counts were rescaled for comparison and analysis. All absorbance and fluorescence measurements were background corrected with a blank 100 mM NaCl solution. All measurements were made in triplicate. Reported results are averages and standard deviations of the triplicate measurements.

$(GT)_N$-SWNT Stability Experiments

We tested the stability of all $(GT)_N$-SWNT suspensions with fluorescence and absorbance spectroscopy. Prior work has shown that DNA-SWNT fluorescence stability directly correlates with DNA polymer stability on the SWNT surface.[2] To rule out the possibility that spontaneous DNA polymer rearrangement or dilution effects contribute to the large increase in nanosensor fluorescence we observed for 'short' sequences, we measured the time-dependent fluorescence stability of all $(GT)_N$-SWNT suspensions with near infrared fluorescence spectroscopy. The fluorescence spectra of all $(GT)_N$-SWNT suspensions were collected for a period of > 2 hrs. immediately following dilution to 5 mg/L in 100 mM NaCl. Most $(GT)_N$-SWNT suspensions exhibit stable fluorescence ($\Delta F/F_0 < -15\%$) with the exception of $(GT)_4$-SWNT, which shows

higher degree of fluorescence instability ($\Delta F/F_0$ = -40%) (Figure S5). Importantly, all sequences exhibit a decrease in intensity that is over an order of magnitude less than the fluorescence increase observed in response to both analytes (Figure S5) suggesting that nanosensor response to analytes arises from specific molecular interaction between $(GT)_N$-SWNT and the analyte and does not arise from volume or dilution effects. The differences in time-dependent fluorescence modulation exhibited by each suspension, as shown in Figure S5, suggests that polymer length affects the base stacking stability of the $(GT)_N$-SWNT suspensions with an apparent instability for N = 4.

Absorbance measurements were also carried out to study the stability of different $(GT)_N$ polymers on SWNT. After synthesis of each $(GT)_N$-SWNT construct, excess ssDNA was removed from the colloidal suspension (Amicon Ultra 100kDA MWCO), and absorption spectra were recorded with a UV-VIS-NIR spectrophotometer. The filtered suspension was then left to incubate at room temperature for 1 week (7 days). After 1 week, absorbance spectra were again collected for each $(GT)_N$-SWNT construct and compared to the sample's initial absorbance. Absorbance values near 260 nm, the DNA absorbance peak, reveal that negligible ssDNA polymer desorption occurs from $(GT)_N$-SWNT constructs within the 1-week timeframe, with the exception of $(GT)_4$-SWNT that shows appreciable $(GT)_4$ polymer desorption from the SWNT surface (Figure S6). Our results suggest that $(GT)_N$ sequences with N>4 form stable non-covalent conjugates with SWNT. For $(GT)_4$-SWNT, we observe a significant increase in absorbance at ~260nm (presumably due to absorbance in the sample filtrate from desorbed DNA). We further note that sequences shorter than $(GT)_4$ did not enable suspension of SWNT. These results provide further evidence for colloidal stability of $(GT)_6$-SWNT, the ultrasensitive dopamine and norepinephrine nanosensor.

Analyte fluorescence response measurements

All neurotransmitters were purchased from Sigma-Aldrich. For neurotransmitter response measurements, we collected fluorescence from 198 µL volumes of suspensions (5 mg/L SWNT concentration) before and after addition of 2 µL of 10 mM solutions of each analyte (for 100 µM final analyte concentration in each well). For dose response curves, analyte stock concentrations were prepared so as to obtain the target concentration in each well upon addition of the 2 µL volumes. Responses to drugs were measured in the same manner. We used 96-well plates (CORNING, 200 µL total volume per well) for screening experiments. Analytes were incubated for 5 minutes before taking post-analyte fluorescence measurements. Responses were calculated for the (9,4)-SWNT chirality peak (~1127 nm center wavelength) as $\Delta F/F_0 = (F-F_0)/F_0$, where F_0 is fluorescence before analyte addition and F is fluorescence after analyte addition and following a 5-minute incubation period. Peak heights (amplitudes) at center wavelengths corresponding to known SWNT (n,m) chiral index in the convoluted spectra are used for all $\Delta F/F_0$ calculations (Figure 1e). Dose-response measurements were fitted to Hill equation, from which dissociation constants were evaluated.[3,4] All measurements were made in triplicate. Reported results are averages and standard deviations of the triplicate measurements. To measure dopamine response of $(GT)_6$-SWNT in DMEM (Dulbecco's) supplemented with 10% Fetal Bovine Serum (FBS) (Gibco, ThermoFisher Scientific), we diluted the as made suspension to 5 mg/L SWNT concentration in the media and allowed 1 hr. incubation at room temperature. Dopamine response was measured as described above. The same procedure was used for artificial cerebrospinal fluid (ACSF) (119 mM NaCl, 26.2 mM $NaHCO_3$, 2.5 mM KCl, 1mM NaH_2PO_4, 1.3 mM $MgCl_2$, 10 mM Glucose, 2 mM $CaCl_2$).

Single Molecule TIRF Experiments

We used visible fluorophore (Cy5) tagged single strand DNA, Cy5-$(GT)_6$ and total internal reflection fluorescence (TIRF) to show that ssDNA adsorbed on SWNT surface are resistant to degradation by nucleases. To do this, we dissolved biotinylated-Cy5-tagged $(GT)_6$ (referred to as Cy5-$(GT)_6$ in this study) (Integrated DNA Technologies) in 100 mM NaCl (nuclease free) by gentle shaking at 50 RPM (Waverly S1C-E) for 30 minutes, then diluted it to 150 pM concentration. Cy5-tagged $(GT)_6$-SWNT suspensions (referred to as Cy5-$(GT)_6$-SWNT in this study) were prepared as described previously, and spin-filtered with 100 kDa Amicon filters (Ultra-0.5mL Centrifugal Filter) 10 times with nuclease-free water to remove free (unsuspended) $(GT)_6$. The SWNT concentration of the resulting supernatant was measured and the solution diluted to 0.2 mg/L SWNT concentration. S1 nuclease (Promega) was diluted using 1x reaction buffer to 250 nM. We used 6-channel slides (ibidi μ-Slide VI 0.5 Glass). Prior to use, each channel was washed by adding 100 μL of 100 mM NaCl to one end and removing 60 μL on the opposite end. The addition of any subsequent solution was immediately followed by the removal of an equal volume of solution at the other end of the channel. In all subsequent steps, substrates were added in 50 μL volumes, and channels flushed with 50 μL solution (100 mM NaCl) to remove unbound substrates post-incubation. First, 0.25 mg/mL of biotinylated Bovine Serum Albumin (BSA-Biotin) and 0.05 mg/mL NeutrAvidin (ThermoFisher Scientific) were added to each channel and incubated for 5 minutes. Non-specific adhesion afforded labeling of the glass surface with BSA-Biotin-NeutrAvidin complexes. Next, Cy5-$(GT)_6$ or Cy5-$(GT)_6$-SWNT were incubated in experimental channels for 5 minutes. Biotin-Cy5-$(GT)_6$ would bind to surface immobilized BSA-Biotin-NeutrAvidin complexes through specific biotin-NeutrAvidin interactions. On the other hand, non-specific adhesion between SWNT surface and

BSA/Neutravidin proteins affords immobilization of the nanosensor (Figure S9). After DNA or SWNT-DNA immobilization, each channel was incubated for 15 minutes in 250 nM S1 nuclease and rinsed with 50 μL NaCl solution to remove degraded DNA. All images were collected with laser excitation at 642 nm, a 655 nm LP emission filter, TIRF angle of 65.35^{o}, and exposure time of 1000 ms (Zeiss Elyra PS.1). The channels were imaged pre and post nuclease incubation. A negative control for each ibidi slide involved using 100 mM NaCl solution in place of DNA or DNA-SWNT. A second negative control used incubation in 100 mM NaCl solution in place of S1 nuclease (Figure S9). The acquired images were processed in MATLAB. An algorithm removed dead pixels and background noise before the image underwent thresholding to obtain a binary image. A built-in function quantified the number of Cy5 fluorophores (spot count) present per field of view. Approximately 25 fields of view were acquired per channel, and each channel experiment was conducted in triplicate. Spot counts for each channel were averaged over the 25 fields of view and the percentage change computed for each channel using pre and post nuclease incubation.

Surfactant-induced solvatochromic shift experiments

We used sodium cholate (SC) (Alfa Aesar) for surfactant displacement experiments. SC solutions was prepared in deionized water and aliquots were added to each well of a 96-well plate for final SC concentrations of 0.25 wt.% for time-resolved experiments and 1 wt.% for steady-state experiments. For time-resolved solvatochromic shift experiments, spectra were collected at 1 s intervals and SC was added 10 s after start of acquisition to obtain 0.25 wt.% SC in each well. Each acquisition lasted between 2 and 5 minutes and SC was allowed to diffuse passively through the well during acquisition. For analyte incubated wells, the wells were spiked

to final analyte concentrations of 10 μM for time-resolved experiments or 100 μM for steady-state experiments. Analytes were allowed to incubate for 5 minutes before addition of SC to a final concentration of 0.25 wt.% or 1 wt.%.

$(GT)_6$-SWNT Raman Measurements

Raman spectra were acquired on a Horiba LabRAM HR Raman microscope. All samples were excited with a 532 nm laser line (50 mW) through a 20x objective and the Raman spectra were collected in a backscattering geometry from 200 μL volume 96-well plates. For all experiments, $(GT)_6$-SWNTs were prepared to a concentration of 20 mg/L in 100 mM NaCl. Stock solutions containing dopamine (DA), norepinephrine (NE) and tyramine (TY) were added to each well for a final analyte concentration of 100 μM. Sodium cholate (SC) was added to select samples for a final concentration of 0.5 wt.% in each well. In measurements containing analytes and SC, the analyte was added to the $(GT)_6$-SWNT solution first and allowed to incubate for 1 minute before SC was added.

Molecular dynamics simulations

Atomistic simulations were conducted to investigate ssDNA-SWNT nanosensors with and without added dopamine analyte. In all simulations, conjugates of (9,4) SWNT with $(GT)_{15}$ and $(GT)_6$ polymers were prepared. (9,4) SWNT segments, 39 Å or 66.73 Å in length, were built in VMD.[5] Conjugates of $(GT)_6$ polymers with two other SWNTs were also examined. An analogous (9,4) SWNT segment of the opposite handedness, also 39 Å in length, was built by transforming the initially built (9,4) SWNT into its mirror image. Separately, a (6,5) SWNT, 53

Å in length, was built in VMD.[3] The initial configurations of $(GT)_{15}$ and $(GT)_6$ ssDNA polymers were built in Material Studio with nucleotides arranged to form helical conformations with radii several Ångstroms wider than the radius of the (9,4) SWNT. The helical DNAs were positioned to wrap SWNTs, with ssDNA bases not pre-adsorbed on the SWNTs surfaces. The length of the SWNT was selected to result in optimal SWNT surface coverage by the adsorbed $(GT)_{15}$ ssDNA via base stacking, which prevents excessive lateral ssDNA diffusion on SWNT. The prepared ssDNA-SWNT conjugates were solvated with TIP3P water and neutralized with 0.1 M NaCl with solvate and ionize VMD plugins, respectively.[5] In simulations of DNA-SWNT conjugates with dopamine, two dopamine molecules were placed ~10 Å away from SWNTs into pre-relaxed systems prepared without dopamine. The final systems contained approximately 11,000 atoms.

The systems were described with CHARMM36 and CHARMM general force field (dopamine) parameters.[6–8] MD simulations were performed with NAMD2.11 package.[9] All simulations were conducted with Langevin dynamics (Langevin constant γLang = 1.0 ps^{-1}) in the NpT ensemble, where temperature and pressure remained constant at 310 K and 1 bar, respectively. The particle-mesh Ewald (PME) method was used to calculate Coulomb interaction energies, with periodic boundary conditions applied in all directions.[10] The time step was set to 2.0 fs. The evaluation of long range van der Waals and Coulombic interactions was performed every 1 and 2 time steps, respectively. After 1,000 steps of minimization, solvent molecules were equilibrated for 2 ns around the DNA and SWNTs, which were restrained using harmonic forces with a spring constant of 1 kcal/(mol $Å^2$). Next, the systems were equilibrated in 250 ns production MD runs, with restraints applied only on the edge SWNT atoms.

To analyze the electrostatic potential created by the surroundings at the SWNT surface, we computed potential energy maps at SWNT surfaces for several configurations of DNA-wrapped

SWNTs. In each configuration, selected from equilibration MD trajectories, SWNT and DNA atoms were restrained with a hard (1.0 kcal/mol/Å^2) and soft (0.1 kcal/mol/Å^2) harmonic restraint, respectively, and simulated for 1 ns. We evaluated the potential energy map at the SWNT surface by averaging electrostatic potential energy contributions and Lennard-Jones contributions from 1 ns simulations of restrained systems. The electrostatic potential energy of each SWCNT atom was computed by setting its charge to $q = -1e$ for the purpose of evaluating the electrostatic potential energy (in 1 ns simulations, each atom had the charge $q = 0$). The average potential energy of each carbon atom in its environment was evaluated with the NAMDEnergy plugin in VMD (each 1 ns trajectory resulted in 500 potential energy data points).[5]

Free energy calculations

The free energy landscape (Figure 3e) was obtained through replica exchange MD (REMD) simulation of a $(GT)_6$-SWNT system solvated in $3.63 \times 3.63 \times 4.92$ nm^3 box, containing 6,605 atoms. The box contained 1,881 water molecules, modeled using TIP3P model. In addition to Na^+ counterions neutralizing the system, 36 Na^+ and Cl^- ions were included to match the physiological salt concentration in the experimental system. Periodic boundary conditions were imposed in all dimensions, and PME method was used to calculate long-range electrostatics. Additionally, both ends of SWNT were in contact with their periodic images. Energy minimization and 100 ps of heating (NVT) were performed to reach the starting temperature of 310 K. To perform REMD simulations in NVT ensemble, 54 replicas and a 290-727.4 K temperature range were chosen to maintain exchange acceptance ratios around 25% with 2 ps exchange time. The total REMD simulation time was 54×270 ns (per replica) = 14.58 μs. The

simulation time step was 2 fs and trajectories were extracted every 2 ps. Therefore, 135,000 configurations per replica were collected. The last 80,000 (160 ns) configurations of room temperature replica were analyzed to obtain the free energy landscape.

To generate the free energy landscape shown in Figure 3e, two independent order parameters of the $(GT)_6$ structure were calculated from the obtained system configurations: 1) end-to-end distance of DNA polymer (the z-distance between centers of mass of the first guanine and last thymine residues; z coordinate aligns with the long axis of the CNT); and 2) Root mean square deviation (RMSD) of phosphorous atoms of the DNA backbone, compared to the configuration these atoms have in the ideal left-handed helix of $(GT)_6$ wrapping SWNT. The probability distribution function ($P(x, y)$) of these two order parameters were calculated and combined to generate free energy ($\Delta F(x, y)$) according to the formula:

$$\frac{\Delta F(x,y)}{k_B T} = -\ln\left(\frac{P(x,y)}{P_{max}}\right)$$

In above formula, P_{max} is the maximum value of $P(x, y)$. Figure 3e was obtained at 300 K by calculating two-dimensional free energy landscape according to the above formula, where x and y represent end-to-end distance and the RMSD of left-helix ssDNA wrapping CNT, respectively.

QM/MD simulations

Quantum mechanics/molecular dynamics (QM/MD) simulations were performed for systems containing SWNT, $(GT)_2$ DNA, Na^+ counterions, with or without dopamine, all described quantum mechanically, and TIP3P water, described classically. The systems examined on the QM/MD level were extracted from the well-equilibrated classical MD simulation of the $(GT)_6$–

SWNT system with dopamine trapped in binding site 2 (Figure S20). Since $(GT)_6$ can stably host Na^+ ions, separate simulations were performed for the systems with and without the hosted Na^+ ions. All extracted systems were solvated and equilibrated in 2 ns classical MD simulations, where all species, except water, were restrained with the harmonic restraint (1.0 kcal/mol/Å^2). The initial configurations of QM/MD simulations were obtained from the final configurations of the above classical MD simulations, in which the water box was cut into a sphere of 28 Å radius.

The QM/MD simulations were performed using TeraChem software (Terachem). The quantum parts of the system were described at the ωB97X/6-31G** level, with dispersion corrections (DFT-D2).[11,12] We used an X-matrix tolerance of 10^{-4}, and a wave function convergence threshold of 10^{-4}. The MD simulations were performed at T = 310 K, using the Langevin dynamics with a damping coefficient of γLang = 1 ps−1 and a time step of 1 fs. No periodic boundary conditions were used; the system was simulated within a water droplet (Figure S18). Atomic charges of the quantum parts of the systems were calculated using the Mulliken population analysis.

Electron and hole wavefunctions in periodic square wells

To approximate the effect of periodic potentials along the SWNT surface on the exciton relaxation, we examined the behavior of negatively (electrons) and positively (holes) charged particles' wavefunctions in periodic square wells, using the Kronig-Penney model. Figure 4h plots the probability densities of electrons and holes (squared wavefunctions). The periodic energy wells are centered at 0 J and their valleys and peaks occur at -1.602×10^{-20} J and 1.602×10^{-20} J, respectively, to roughly match the periodic potential energies created at the SWNT

surface by the ring $(GT)_6$ ssDNAs. The wavefunction energies were chosen as -0.641×10^{-20} J. The periodic square wells are 1.5 nm in length, also matching the periodic potential shape created by the ring DNAs.

Supplementary Figures

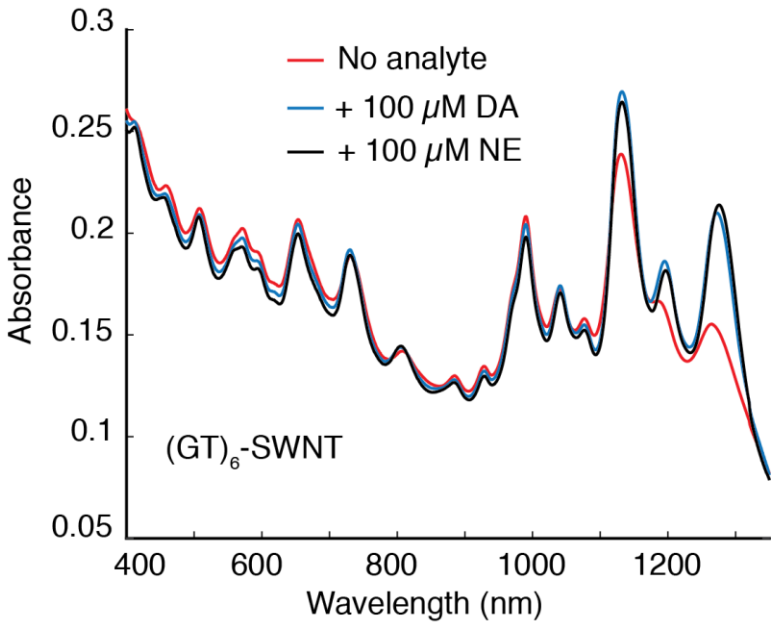

Figure S1. Absorption spectra of $(GT)_6$-SWNT before and after analyte addition. Absorbance of $(GT)_6$-SWNT before (red trace) and after (black and blue traces) addition of 100 μM dopamine (DA) and norepinephrine (NE) shows little change at 721 nm, the excitation wavelength used for all fluorescence measurements in this study. E_{22} transitions are unaffected whereas addition of analytes is observed to reduce transition bleaching in the E_{11} region of the spectrum.

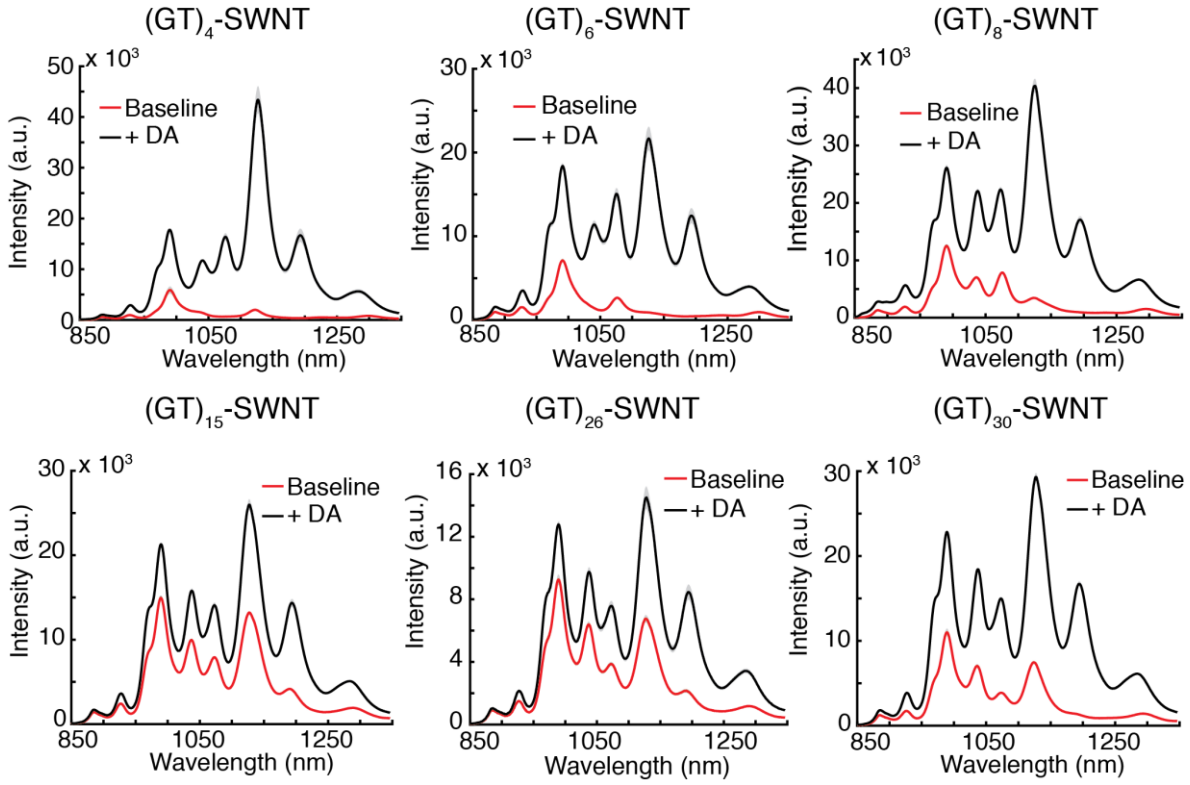

Figure S2: Fluorescence spectra of three short (N=4, 6, 8) and long (N=15, 26, 30) of $(GT)_N$-SWNT suspensions. Fluorescence before addition (red trace) and after (black trace) addition of 100 µM of dopamine (DA) is shown. Mean traces and standard deviation (gray band) from N=3 technical replicates are presented.

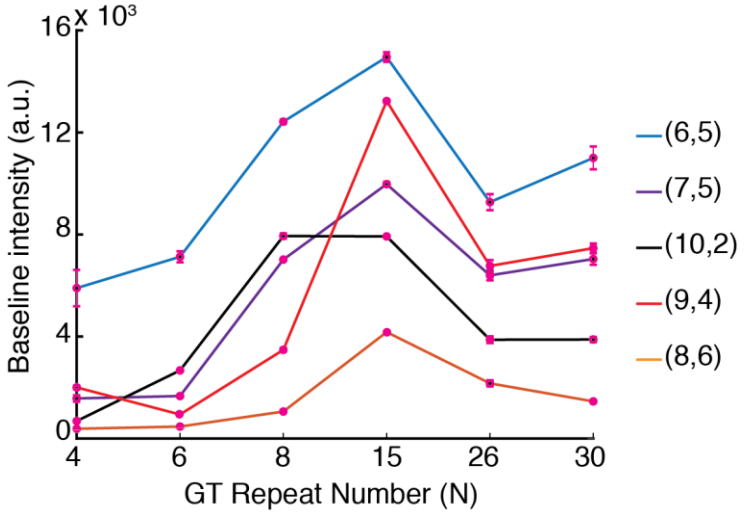

Figure S3: Baseline fluorescence intensity of $(GT)_N$-SWNT before any analyte addition shows a diameter dependent fluorescence quenching. SWNT chiralities bigger than the (6,5) species show the lowest baseline fluorescence that increases with increasing N. Error bars are standard deviation of N=3 technical replicates.

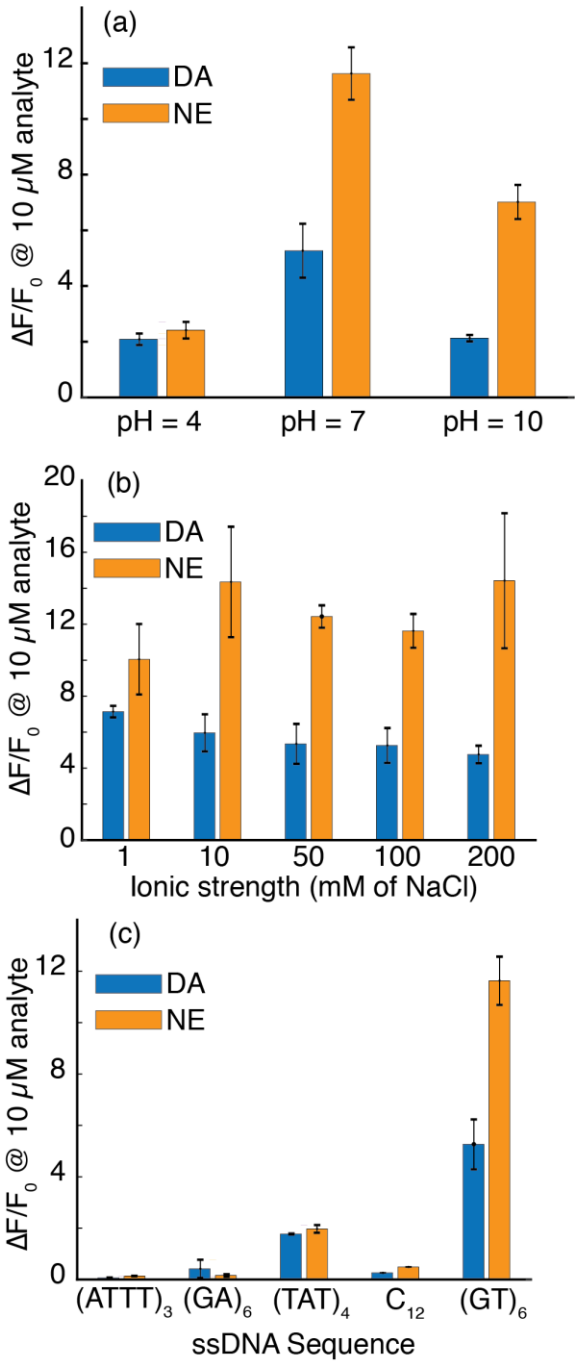

Figure S4. Nanosensor stability over varying ionic strengths and pH. (a) Nanosensor response to dopamine and norepinephrine is observed for a wide range of solution pH, with maximal response occurring at physiological pH of 7. (b) Nanosensor response to dopamine and norepinephrine under NaCl ionic strength conditions that vary over two orders of magnitude. (c) Response to dopamine and norepinephrine is GT sequence specific. Experiments with other 12-mer constructs show marginal $\Delta F/F_0$ compared to $(GT)_6$. Error bars are standard deviation of N=3 technical replicates. All $\Delta F/F_0$ are reported for the peak intensity change at the center wavelength of (9,4) SWNT chirality (~1127 nm) from the convoluted fluorescence spectra.

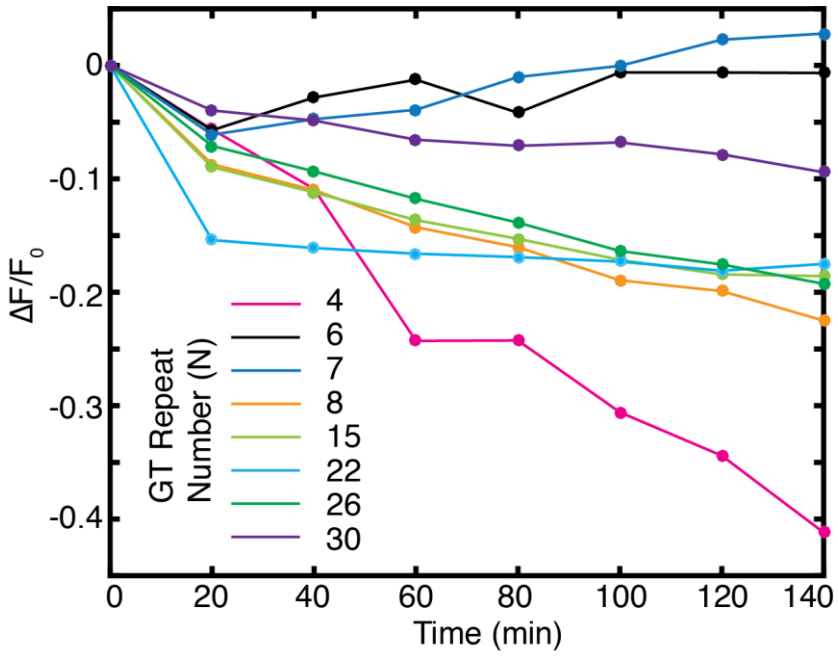

Figure S5. Change in $(GT)_N$-SWNT fluorescence intensity as a function of time. All suspensions were diluted to a SWNT concentration of 5 mg/L in 100 mM NaCl and their fluorescence spectrum was monitored over two hours immediately following dilution.

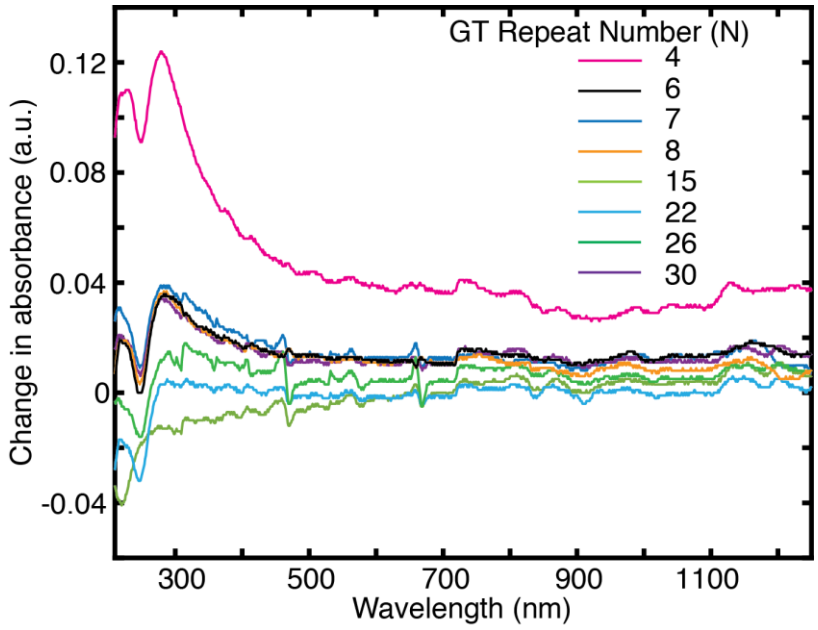

Figure S6. DNA desorption from SWNT over the course of 1 week. Change in absorbance for $(GT)_N$-SWNT suspensions after 1 week of incubation, indicating the relative instability of the $(GT)_4$-SWNT suspension compared to $(GT)_6$-SWNT and longer. Absorption at 260 nm corresponds to desorbed ss$(GT)_N$ polymer. For more details, see Methods).

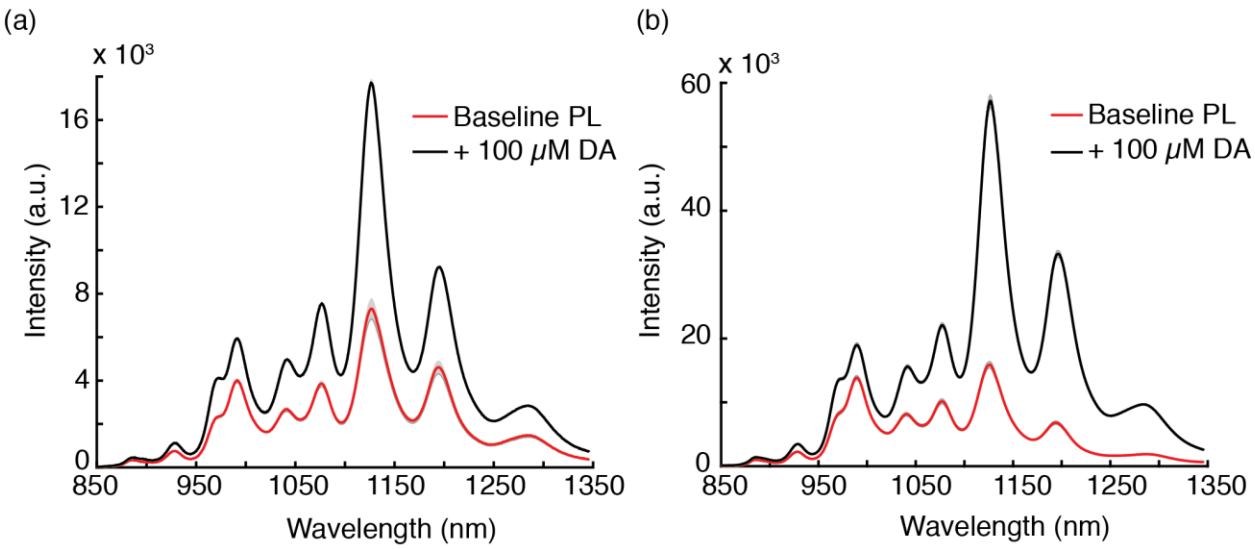

Figure S7: (a) $(GT)_6$-SWNT response to dopamine (DA) after 1-hr incubation in DMEM+10% FBS. $(GT)_6$-SWNT was diluted and equilibrated in DMEM+10% FBS for 1 hr. before dopamine response measurements were taken. (b) Another set of dopamine response experiments were repeated with nanosensors equilibrated in artificial cerebrospinal fluid (ACSF). Data is presented as a mean trace and standard deviation (gray band) from N=3 measurements.

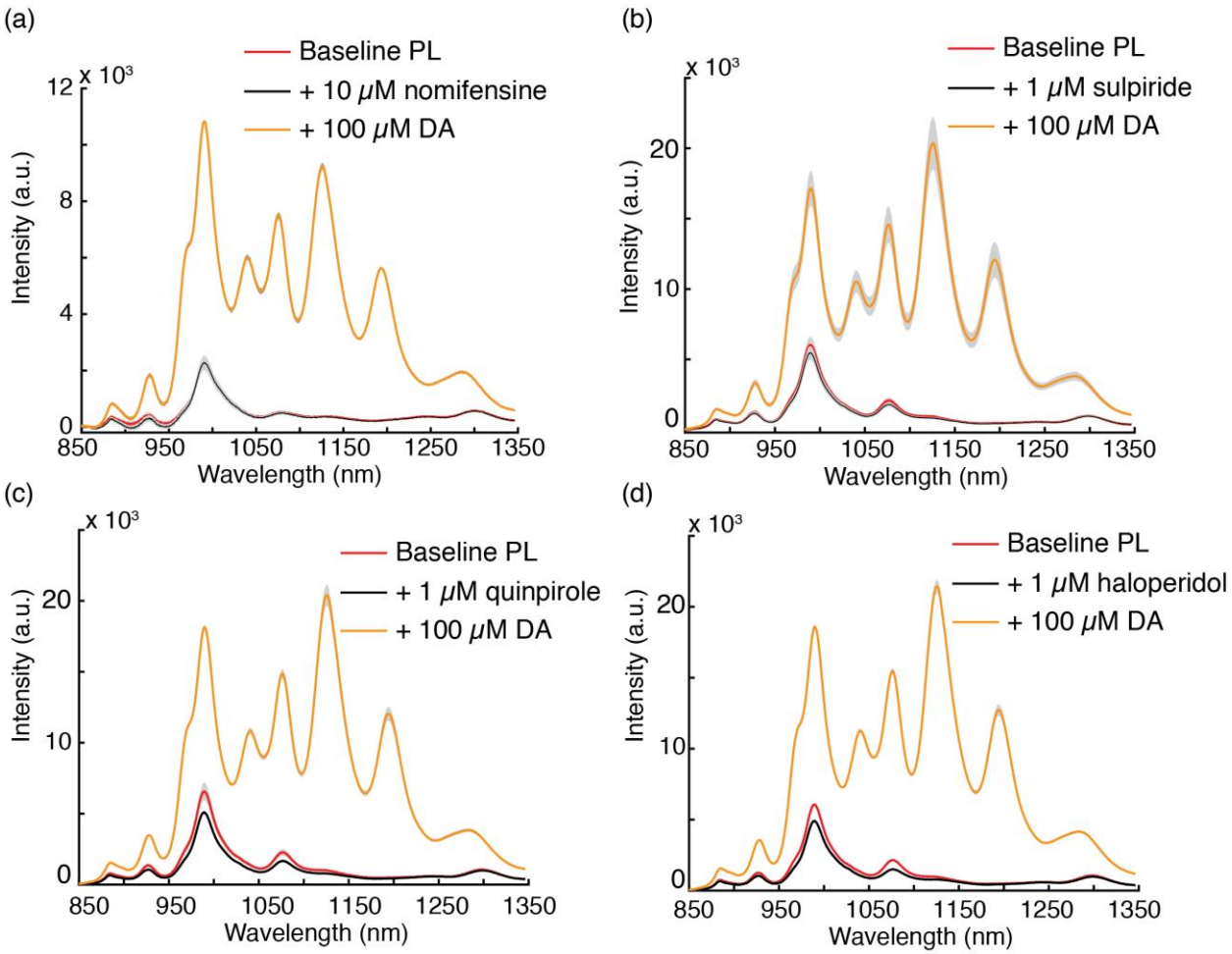

Figure S8: Response of $(GT)_6$-SWNT to various drugs. No response or negligible negative responses are observed for (a) 10 μM of nomifensine and 1 μM each of (b) sulpiride, (c) quinpirole and (d) haloperidol. After incubation in each drug, subsequent responses to 100 μM of dopamine are measured and show no attenuation (orange traces). All traces are presented as mean and standard deviation (gray band) from N=3 technical replicates.

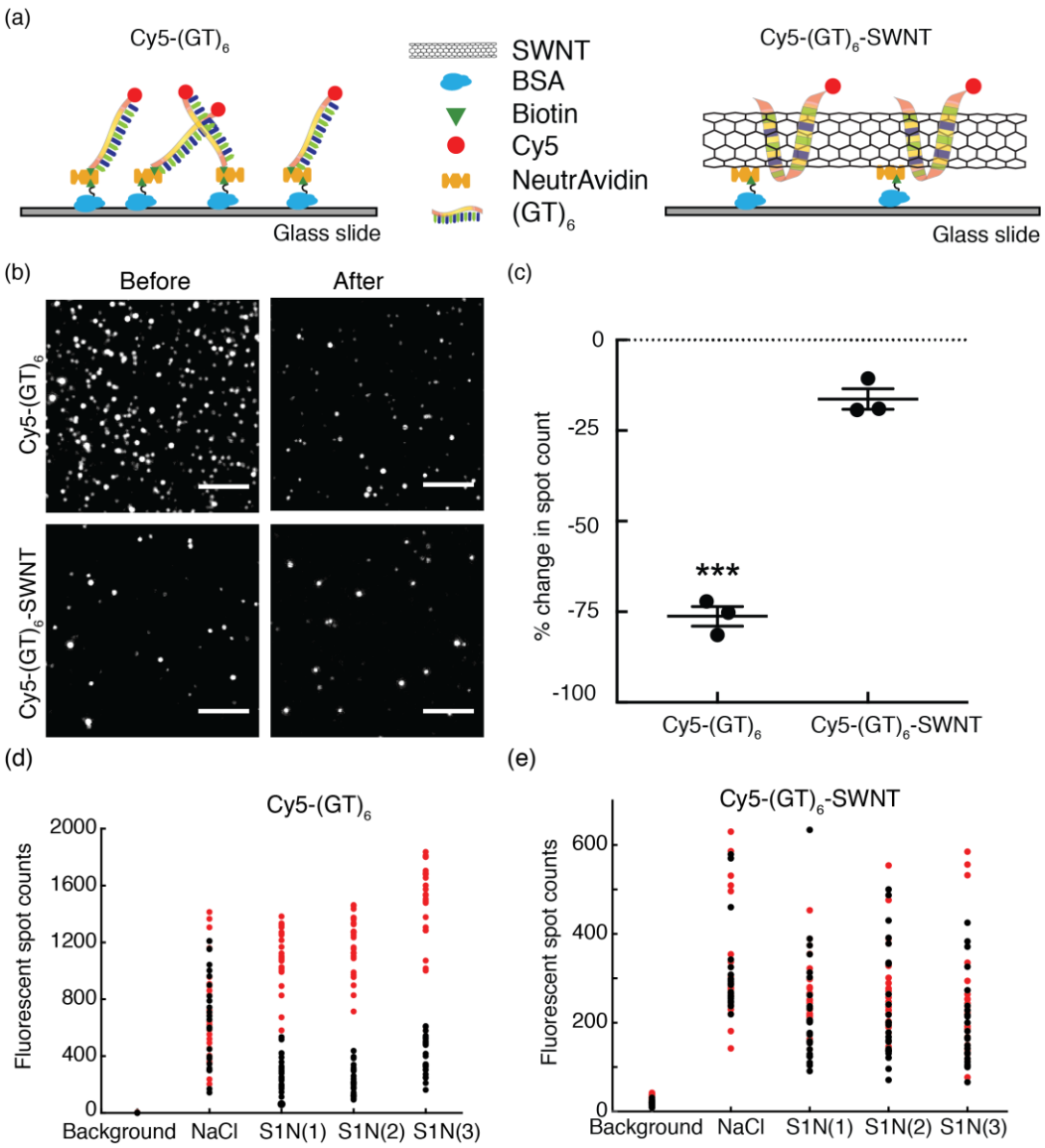

Figure S9: Single molecule TIRF is used to evaluate degradation of ssDNA by S1 nuclease. (a) Cy5-$(GT)_6$ and Cy5-$(GT)_6$-SWNT were surface immobilized on a glass slide (Methods). (b) A representative field of view in a channel with Cy5-$(GT)_6$ (top row) and Cy5-$(GT)_6$-SWNT (bottom row) before and after 15-minute incubation in S1 nuclease. S1 nuclease mediated degradation of ssDNA diminishes Cy5 fluorescence. Scale bars = 5 µm. (c) Percentage change in Cy5 spot count shows $(GT)_6$ adsorbed on SWNT are not degraded as effectively by S1 nuclease compared with free $(GT)_6$ ($p < 0.001$). (d) Scatter plot of spot counts in a control lane treated with 100 mM NaCl (Background) shows negligible non-specific fluorescence. Four channels in which Cy5-$(GT)_6$ are immobilized shows that treatment with 100 mM NaCl has no effect on spot counts (NaCl) and treatment with S1 nuclease (S1N(1), S1N(2), S1N(3)) diminishes spot counts. Each dot represents Cy5 counts from a field of view either before (red) incubation in buffer or nuclease or after (black) incubation in buffer or nuclease, and then (e) repeated with Cy5-$(GT)_6$-SWNT as the substrate.

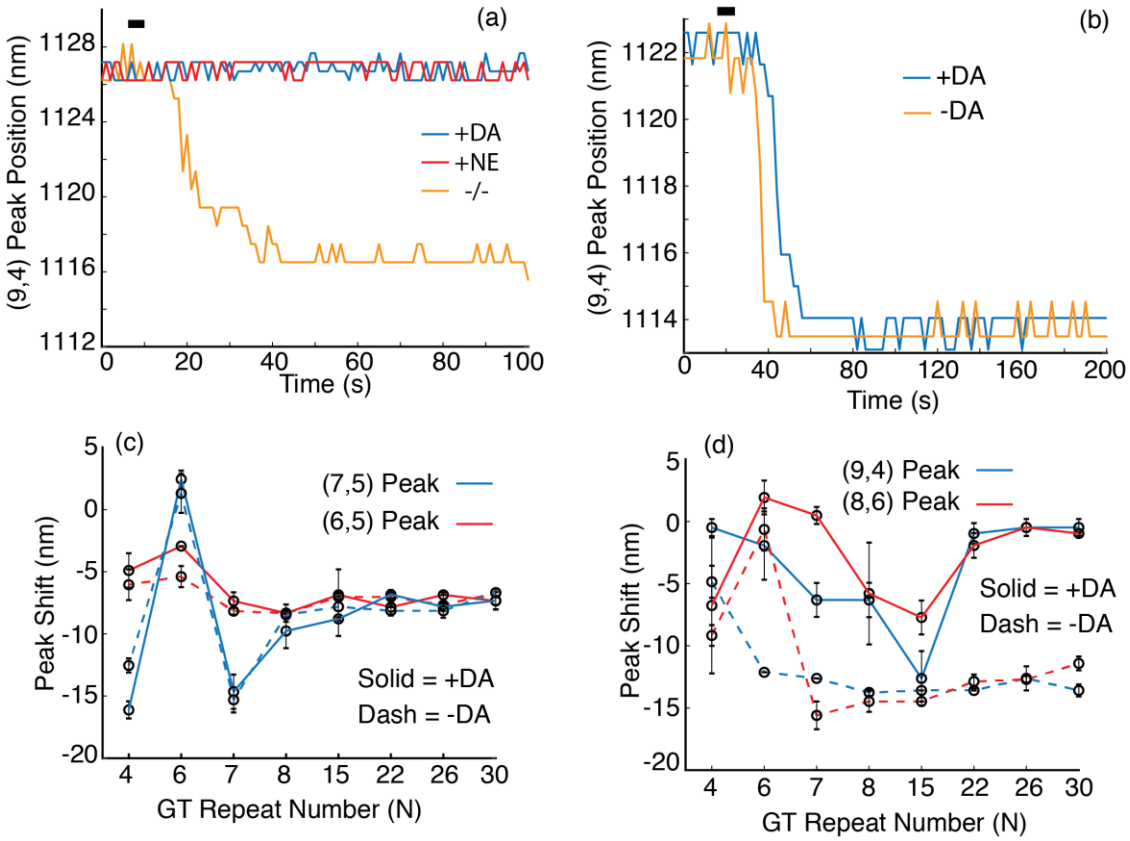

Figure S10. Solvatochromic shifts induced by the addition SC surfactant to ssDNA-SWNT constructs. (a) Shifts caused by 0.25 wt.% SC when no dopamine (DA) or norepinephrine (NE) is present (orange trace) is eliminated in the presence of 10 µM of DA (blue trace) and 10 µM of NE (red trace). Black bar indicates time of SC addition. (b) For C_{12}-SWNT construct, incubation in 10 µM of DA does not eliminate shift caused by 0.25 wt.% SC (c) Peak shifts of the (6,5) and (7,5) chirality with DA (100 µM) (solid trace) and no DA (dash) show analyte induced corona stability is limited for smaller diameter SWNTs, consistent with their diminished $\Delta F/F_0$ in response to DA. (d) On the other hand, bigger diameter peaks (9,4) and (8,6), which exhibit the strongest analyte mediated fluorescence modulation are strongly stabilized by the addition of DA. Peak shifts are computed by as the difference between steady-state (long time behavior) and initial peak positions. Final SC concentrations for (c) and (d) are 1 wt.%. Error bars are standard deviations from n=3 replicates.

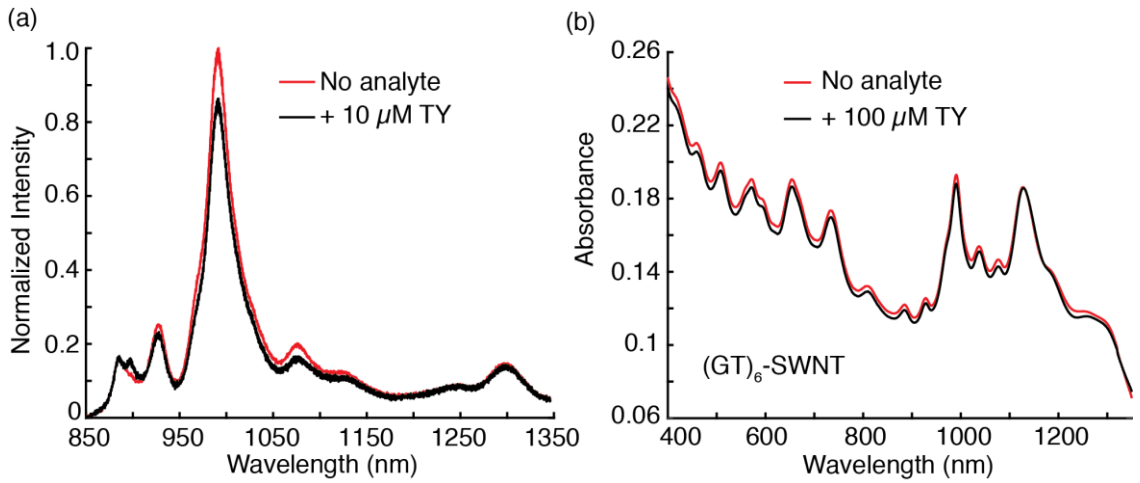

Figure S11. (a) Fluorescence modulation of $(GT)_6$-SWNT upon addition of p-tyramine (TY). Addition of 10 μM TY causes negligible fluorescence modulation of the $(GT)_6$-SWNT construct. (b) Absorbance measurements before (red trace) and after (black trace) addition of 100 μM of TY. Negligible absorption modulations are observed in the E_{11} and E_{22} regions of the spectrum.

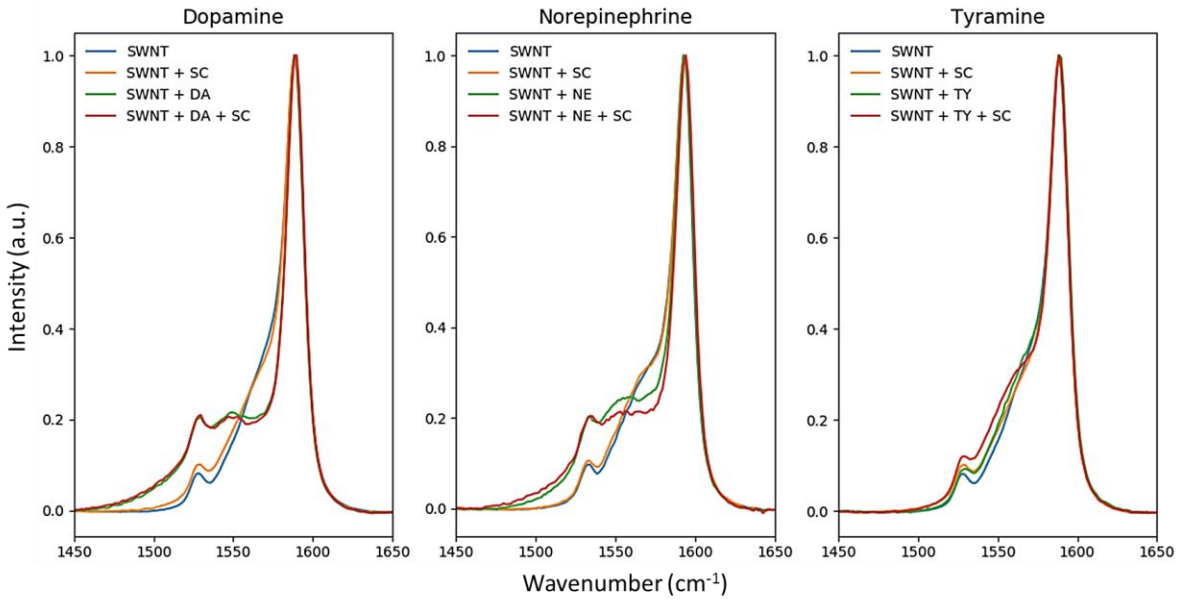

Figure S12. Selective Raman peak broadening of $(GT)_6$-SWNT by dopamine and norepinephrine. The effects on the Raman spectra for $(GT)_6$-SWNT in the G-band region are shown for the addition three analytes. The blue spectra correspond to 20 mg/L of $(GT)_6$-SWNT. Orange spectra contain 20 mg/L $(GT)_6$-SWNT with sodium cholate (SC) added to 0.5 wt.%. Green spectra show $(GT)_6$-SWNT with the respective analyte added to a final concentration of 100 μM after 1 minute of incubation. Both dopamine and norepinephrine produce a strong response in the G^- portion of the spectrum, which is absent from the tyramine measurements. The effect is maintained regardless of the subsequent addition of SC, suggesting the molecular recognition of dopamine and norepinephrine analytes disallows SC adsorption.

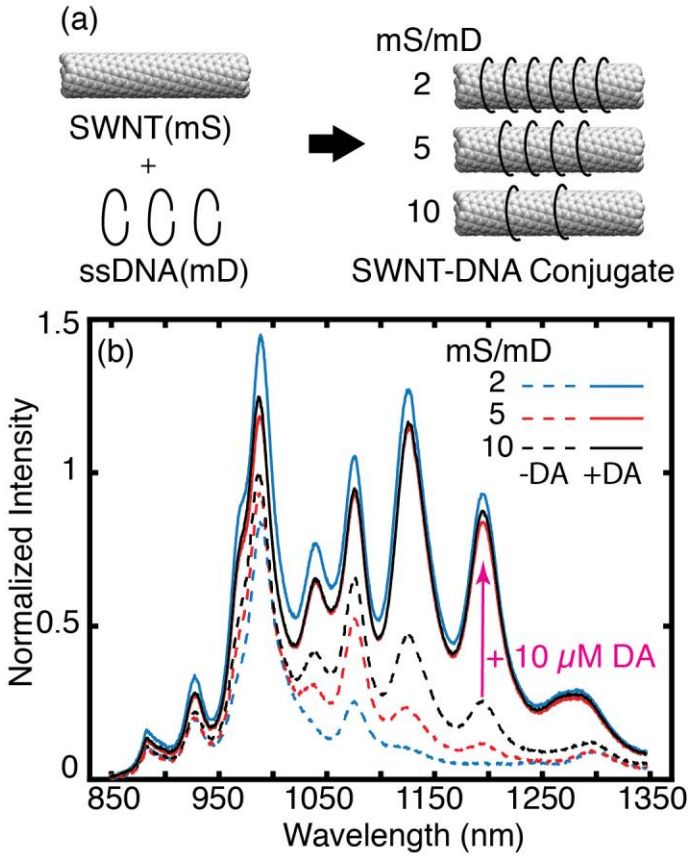

Figure S13. DNA surface coverage of SWNT modulates dopamine binding sites. (a) Preparation of SWNT sensors with varying $(GT)_6$ polymer surface density. The mass ratio of SWNT to ssDNA (mS/mD) is varied to prepare three suspensions with m/n = 2, 5 and 10. (b) Fluorescence spectra of 5 mg/L $(GT)_6$-SWNT samples (dashed plots), with corresponding fluorescence spectra after addition of 10 μM of dopamine (solid plots), normalized to the peak fluorescence intensity observed for the mS/mD=10 sample before addition of 10 μM dopamine.

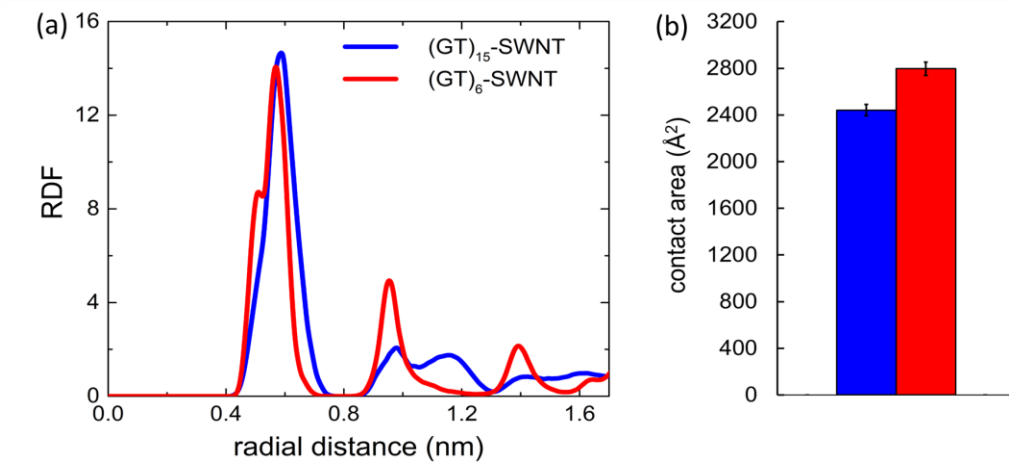

Figure S14. DNA distribution and surface coverage on SWNTs. a) Radial distribution functions of phosphate groups (P-atom) of $(GT)_{15}$ and $(GT)_6$ DNAs on SWNTs, calculated for the last 100 ns of simulations. (b) Contact areas between DNA strands and SWNTs, averaged over the last 100 ns of simulations.

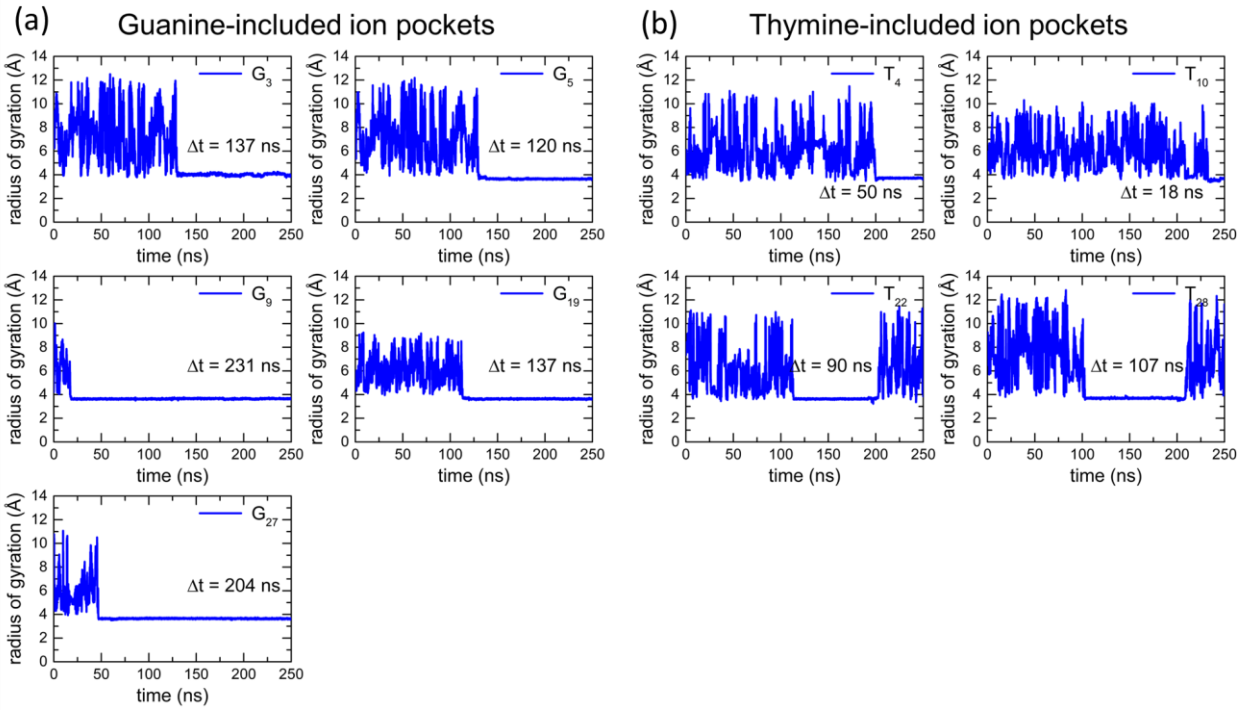

Figure S15. Residence times of Na^+ ions hosted by $(GT)_{15}$ DNAs. (a) Residence times of Na^+ ions hosted by guanine (a) and thymine (b) nucleotides of $(GT)_{15}$ DNA on (9,4) SWNT. The residence times were calculated based on radii of gyration of selected nucleotide atoms and trapped Na^+ ions.

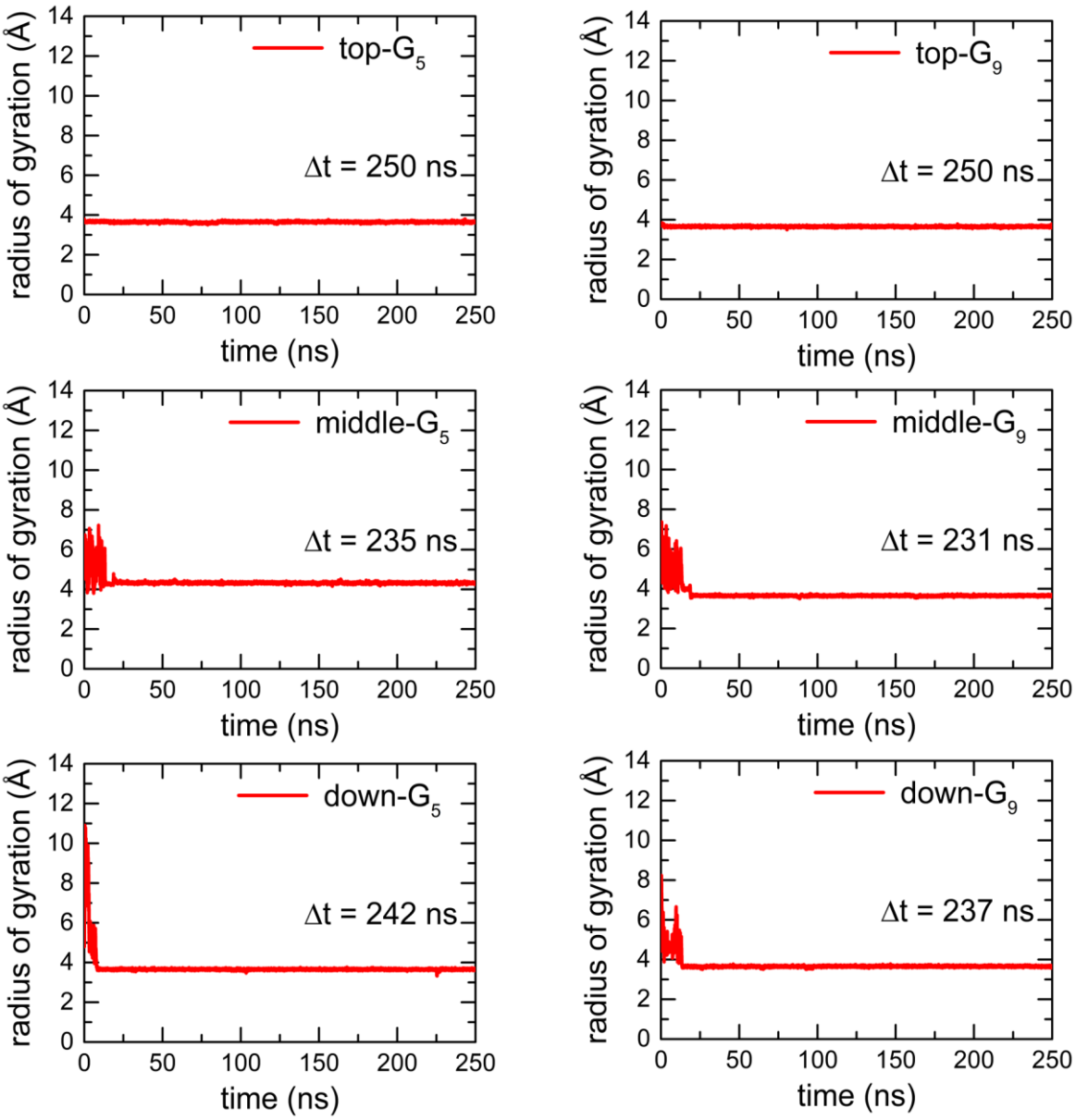

Figure S16. Residence times of Na^+ ions hosted by $(GT)_6$ DNAs. (a) Residence times of Na^+ ions hosted by guanine nucleotides of $(GT)_6$ DNA on (9,4) SWNT. Guanine residues 5 and 9 of every single $(GT)_6$ strand on SWNT hosted Na^+ ions (the system analyzed is shown in Figure 3, and top, middle and down refers to three $(GT)_6$ strands). The residence times were calculated as in Figure S9.

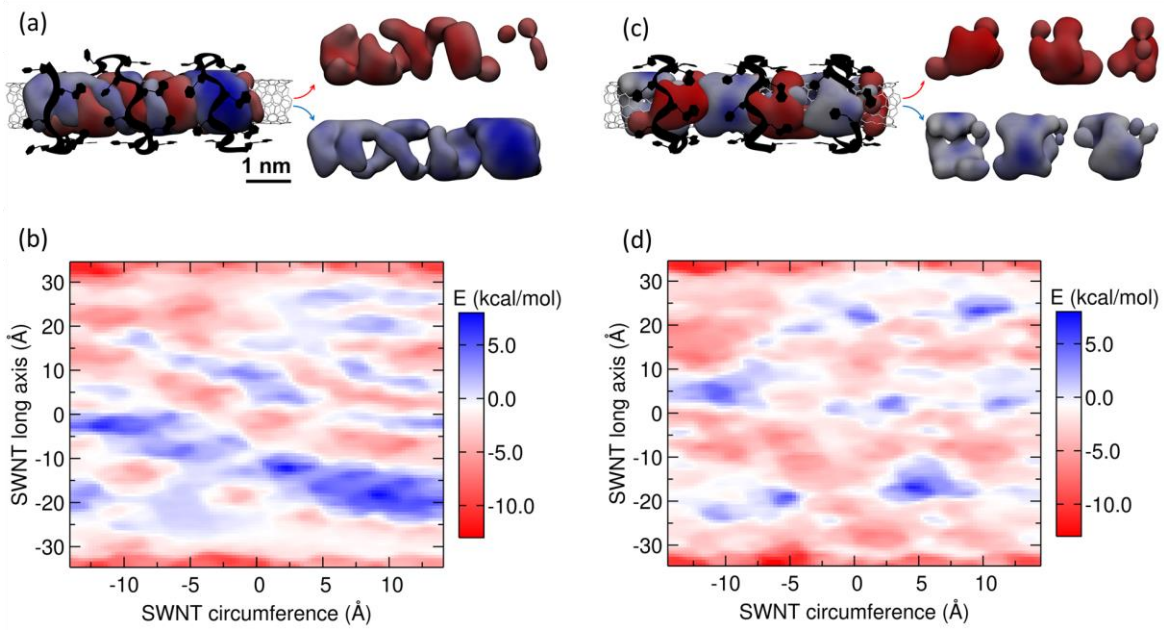

Figure S17. Electrostatic potential pattern at the SWNT surface. (a) The extended electrostatic potential pattern at the SWNT surface of the $(GT)_{15}$-SWNT system. Red and blue regions represent negative and positive potential domains, respectively. For clarity, isolated positive and negative regions are shown separately on the right. (b) Plot of the complete potential energy surface at the SWNT for the system shown in panel a. (c) The localized potential pattern at the SWNT surface of the $(GT)_6$-SWNT system. The color scheme is as in panel a. (d) Plot of the potential energy surface at the SWNT for the system shown in panel c.

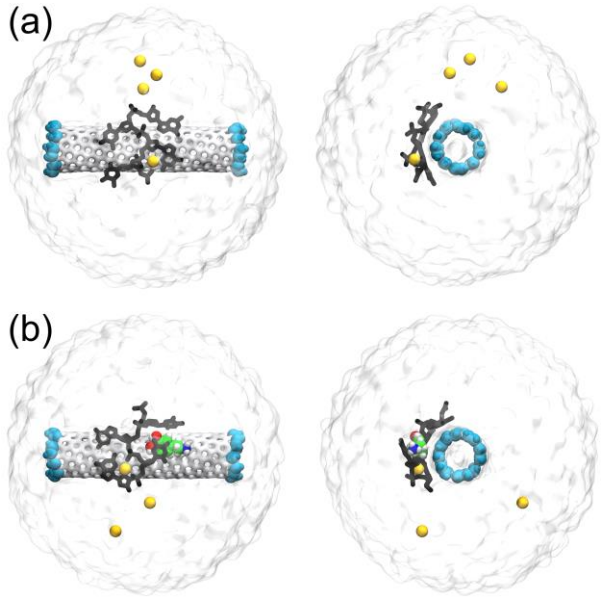

Figure S18. Representative systems examined in QM/MD simulations. (a) $(GT)_2$–SWNT system with one hosted Na^+ ion and three solution Na^+ ions. (b) Dopamine (binding site 2) in the $(GT)_2$–SWNT system, containing three solution Na^+ ions. Classically described water in the

system is shown as a transparent surface. The atoms in the system are shown in yellow (Na), silver (non-terminal SWNT atoms), black (atoms of nucleotides), blue surface (terminal -CH groups capping the SWNT), green (carbon atoms of dopamine), red (O), dark blue (N), orange (P) and white (H).

6-31g** basis set	systems	Middle-carbons	Edges-carbons	whole SWNT	Nucleic Acid	Na	Cl	Total
	SWNT	+0.35	-0.35	0	-	-	-	0
	SWNT-Na	+0.59	-0.59	0	-	+1	-	+1
	SWNT-Cl	+0.67	-0.67	0	-	-	-1	-1
	SWNT-Na-Cl	+0.81	-0.81	0	-	+1	-1	0
	SWNT-G-non-hosted	+0.77	-0.75	+0.02	-1.02	+1	-	0
	SWNT-G-hosted	+0.69	-0.66	+0.03	-0.76	+0.73	-	0
	SWNT-T-non-hosted	+0.293	-0.258	0.035	-1.035	+1	-	0
	SWNT-T-hosted	+1.05	-1.02	+0.03	-0.90	+0.87	-	0
	SWNT-GT2 (only one-hosted Na)	+0.724	-0.648	+0.076	-3.615 (4 phosphate groups)	3.539	-	0

Table S1. Net charges of different parts of SWNT, SWNT-ion, and SWNT-DNA systems, described in quantum mechanical calculations. The charge is reported in units of *e*, the unit charge. All systems had SWNT, ions, and DNA described quantum mechanically, and the water described classically. The calculation details are described in the methods.

6-31g** basis set	systems	Middle-carbons	Edges-carbons	whole SWNT	Nucleic Acid	DOP	Na	Total
	SWNT-GT2 (only one-hosted Na)	+0.724	-0.648	+0.076	-3.615	-	3.539	0
	SWNT-DOP	+0.28	-0.26	+0.02	-	+0.98	-	+1
	SWNT-DOP-GT2 (**sandwich site** and only one-hosted-Na)	+0.466	-0.383	+0.083	-3.506	+0.950	+2.473	0
	SWNT-no-DOP-GT2 (**Dopamine was removed** and only one-hosted-Na)	+0.596	-0.513	+0.083	-3.583	0	+3.500	0

Table S2. Net charges of different parts of SWNT-DNA systems with and without the dopamine molecule, described in quantum mechanical calculations. All the systems had SWNT, ions, DNA, and dopamine (when present) described quantum mechanically, and the water described classically. The dopamine binding site examined is the binding site 2 of the $(GT)_6$-SWNT system, shown in Figure. S14b.

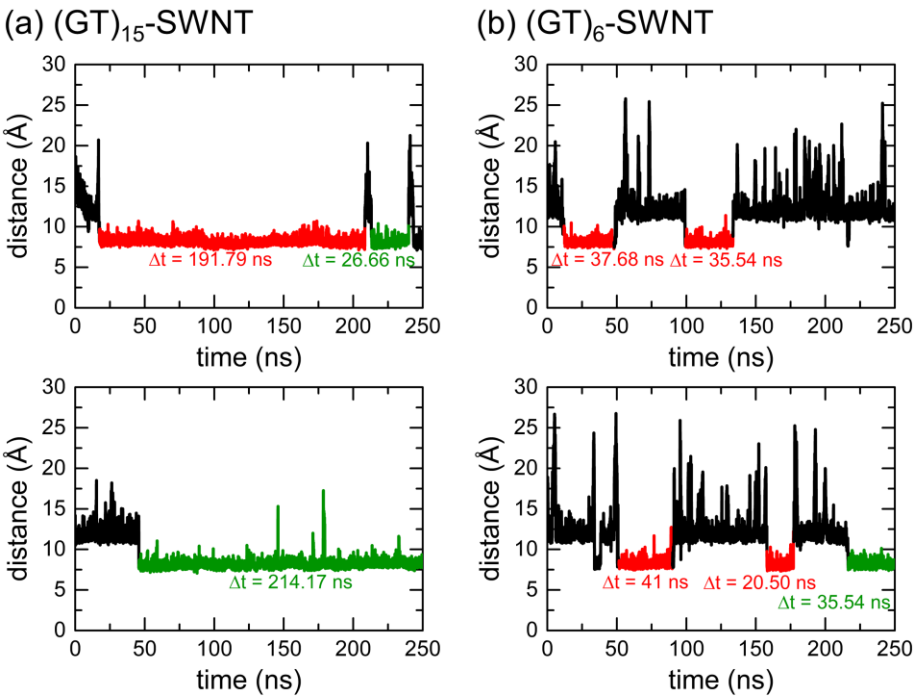

Figure S19. Residence times of dopamine molecules in their binding sites. (a) Residence times of dopamine in $(GT)_{15}$-SWNT systems in binding sites (red) 1 and 2 (green). (b) Residence times of dopamine in $(GT)_6$-SWNT systems in binding sites 1 (red) and 2 (green). Residence times were calculated by tracking the radial distance between the dopamine ring center of mass and the central axis of SWNT. Dopamine binds more stably to $(GT)_{15}$ than to $(GT)_6$.

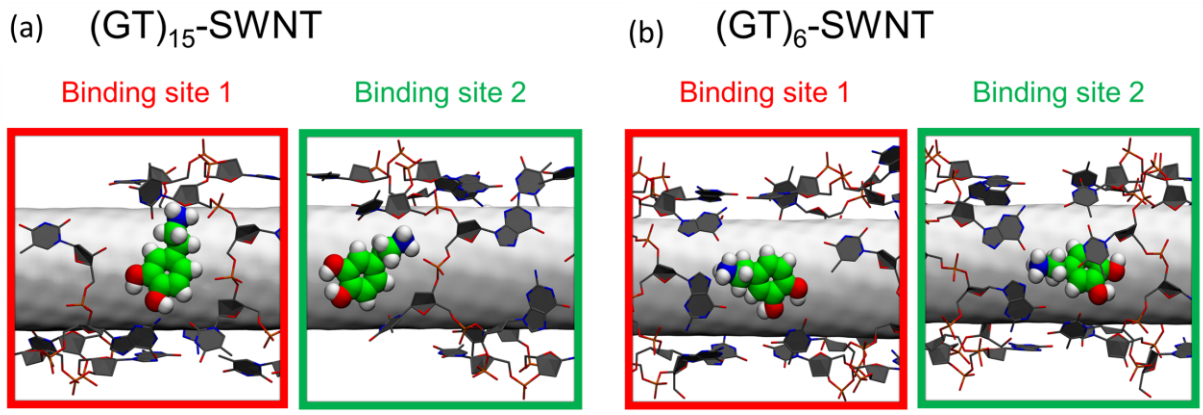

Figure S20. Dopamine binding to DNA-SWNT systems. Two representative binding poses of dopamine (a) in the $(GT)_{15}$-SWNT system and (b) in the $(GT)_6$-SWNT system. Atoms of dopamine are shown in green (C), red (O), blue (N), and white (H). Dopamine opens a space between consecutive bases of $(GT)_{15}$ and binds with its amine group to the DNA phosphate. The helical arrangement of nucleotides in $(GT)_{15}$ allows for the opening of consecutive bases and dopamine insertion. Conversely, the ring arrangement of $(GT)_6$ nucleotides prevents spreading of consecutive nucleotides (which would allow dopamine insertion), and dopamine primarily interacts with bases of neighboring $(GT)_6$ strands in a bridge-like binding mode.

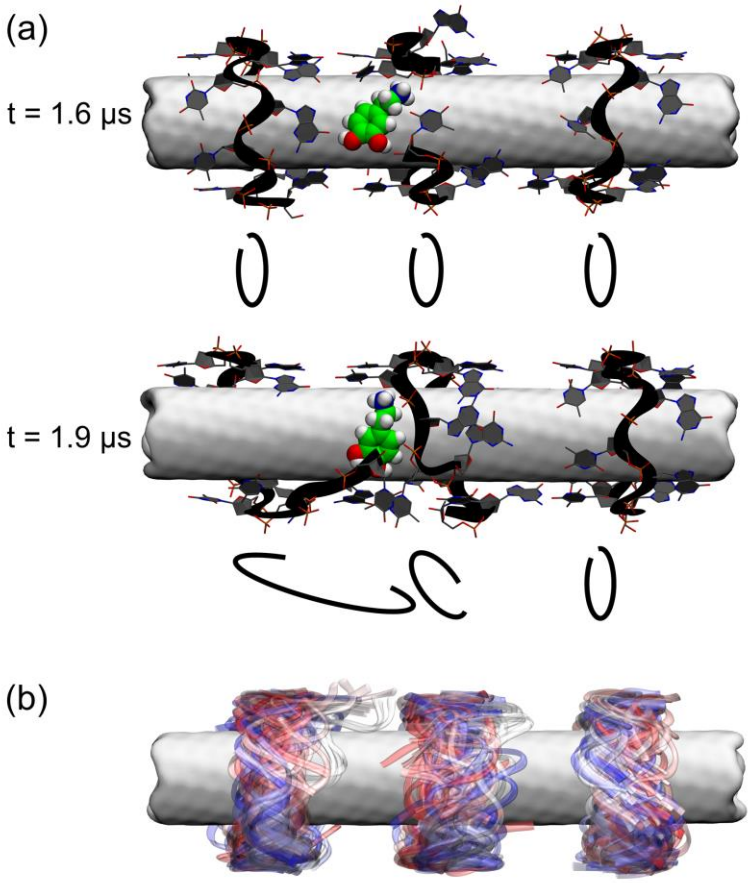

Figure S21. Dopamine adsorption to $(GT)_6$. (a) $(GT)_6$ ring structures become distorted due to dopamine adsorption. Two snapshots of dopamine adsorbed to $(GT)_6$-wrapped SWNTs, after 1.6 μs and 1.9 μs of a classical MD simulation. $(GT)_6$ ring structures become distorted due to the presence of dopamine after 1.9 μs. (b) $(GT)_6$ polymers mainly preserve ring structures in a 4.6 μs long MD simulation. $(GT)_6$ rings occasionally convert to helical conformations, followed by returns to the ring conformations; the largest changes from ring conformations are observed when DNA strands interact directly with dopamine. The backbones of three $(GT)_6$ strands are shown over the course of a 4.6 μs long MD simulation; snapshots were selected every 50 ns. Blue, white, and red colors of the $(GT)_6$ backbone snapshots represent the beginning, the middle and the end of the trajectory.

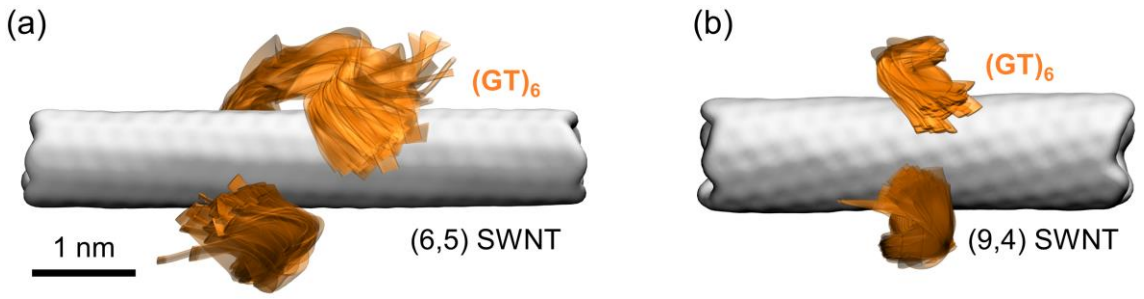

Figure S22. MD simulations of $(GT)_6$ polymers complexed with SWNTs of different diameter and handedness. (a) Conformations of a $(GT)_6$ polymer on a (6,5) SWNT. The $(GT)_6$ strand predominantly adopts a helical conformation. (b) Conformations of a $(GT)_6$ strand on a (9,4) SWNT of an opposite handedness than the (9,4) SWNT explored in Figure 3. The $(GT)_6$ strand predominantly adopts ring-like conformations. SWNTs are shown as gray surfaces, backbones of $(GT)_6$ strand are shown as orange ribbons. Backbones of $(GT)_6$ are aligned, and 80 conformations, assumed every 2 ns in MD simulations, are overlaid. The conformations shown represent the dynamics of $(GT)_6$ in 160 ns MD trajectories.

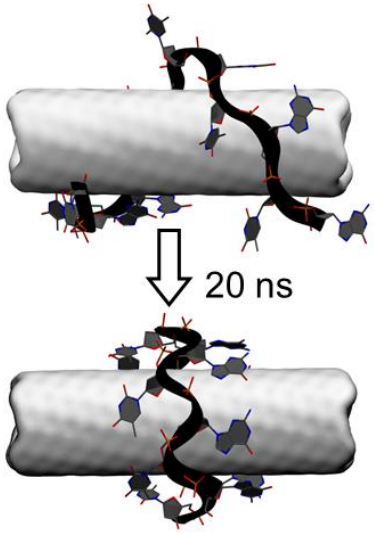

Figure S23. $(GT)_6$ spontaneously assumes a ring-like conformation on a (9,4) SWNT in five independent 200 ns long MD simulations.

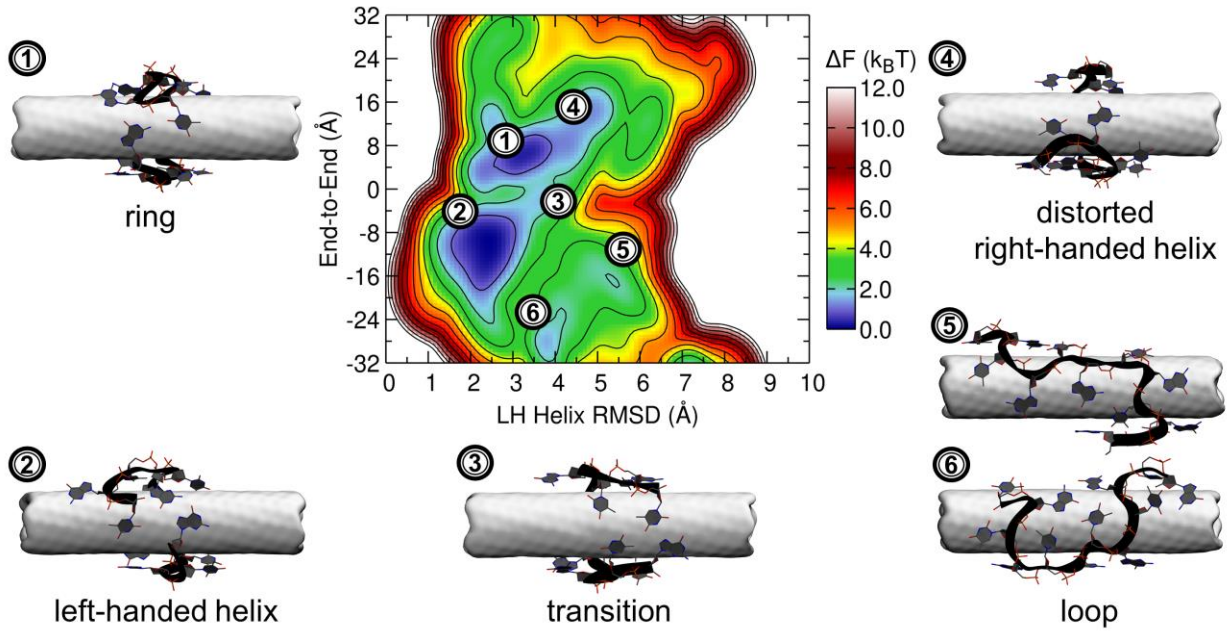

Figure S24. Free energy landscape of $(GT)_6$-SWNT at 300 K on the (9,4) SWNT species. The conformations associated with various free energy minima and a transition state are labeled by indices 1-6. The state labeled by index 3 marks the transition state between free energy minima labeled by indices 1 and 2.

References

1. Salem, D. P. *et al.* Ionic Strength-Mediated Phase Transitions of Surface-Adsorbed DNA on Single-Walled Carbon Nanotubes. *J. Am. Chem. Soc.* (2017). doi:10.1021/jacs.7b09258

2. Landry, M. P. *et al.* Comparative Dynamics and Sequence Dependence of DNA and RNA Binding to Single Walled Carbon Nanotubes. *J. Phys. Chem. C* (2015). doi:10.1021/jp511448e

3. Weiss, J. N. The Hill equation revisited: uses and misuses. *FASEB J.* (1997). doi:0892-6638/97/0011

4. Kurganov, B. I., Lobanov, A. V., Borisov, I. A. & Reshetilov, A. N. Criterion for Hill equation validity for description of biosensor calibration curves. *Anal. Chim. Acta* (2001). doi:10.1016/S0003-2670(00)01167-3

5. Humphrey, W., Dalke, A. & Schulten, K. VMD: Visual molecular dynamics. *J. Mol. Graph.* (1996). doi:10.1016/0263-7855(96)00018-5

6. Huang, J. & Mackerell, A. D. CHARMM36 all-atom additive protein force field: Validation based on comparison to NMR data. *J. Comput. Chem.* (2013). doi:10.1002/jcc.23354

7. Vanommeslaeghe, K. *et al.* CHARMM general force field: A force field for drug-like molecules compatible with the CHARMM all-atom additive biological force fields. *J. Comput. Chem.* (2010). doi:10.1002/jcc.21367

8. Yu, W., He, X., Vanommeslaeghe, K. & MacKerell, A. D. Extension of the CHARMM general force field to sulfonyl-containing compounds and its utility in biomolecular simulations. *J. Comput. Chem.* (2012). doi:10.1002/jcc.23067

9. Phillips, J. C. *et al.* Scalable molecular dynamics with NAMD. *Journal of Computational Chemistry* (2005). doi:10.1002/jcc.20289

10. Darden, T., York, D. & Pedersen, L. Particle mesh Ewald: An N·log(N) method for Ewald sums in large systems. *J. Chem. Phys.* (1993). doi:10.1063/1.464397

11. Grimme, S., Antony, J., Ehrlich, S. & Krieg, H. A consistent and accurate ab initio parametrization of density functional dispersion correction (DFT-D) for the 94 elements H-Pu. *J. Chem. Phys.* (2010). doi:10.1063/1.3382344

12. Grimme, S., Ehrlich, S. & Goerigk, L. Effect of the damping function in dispersion corrected density functional theory. *J. Comput. Chem.* (2011). doi:10.1002/jcc.21759